Microrobotic Platform for Manipulation and Flexibility Measurement of Individual Paper Fibers

P. Saketi, *Student Member*, *IEEE*, A. Treimanis, P. Fardim, P. Ronkanen, P. Kallio, *Member*, *IEEE*

Abstract— This paper introduces a microrobotic platform to manipulate and characterize individual paper fibers. Mechanical characterization of individual paper fibers determines the key parameters which affect the quality of paper sheets. Current laboratory tests are based on bulk paper fiber measurements. This paper presents a microrobotic platform which is able to characterize the flexibility of individual paper fibers directly, not in bulk amount and using indirect estimations. The flexibility of three different pulp samples is measured and the experimental results are reported.

I. INTRODUCTION

The development of micro- and nanorobotics technologies and systems and their demonstration in different application sectors has been very active in the recent years [1]–[5]. Micro- and nanorobotics have provided significant added value to the research of living cells such as oocytes and embryos manipulated in liquid suspension [6]–[8], various adherent eukaryotic cells which need a substrate to grow, bacterial cells and even sub-cellular components and structures [9]–[15]. Other important application areas of micro- and nanorobotic systems are microassembly [16], manipulation of nanoparticles such as carbon nanotubes [17], [18] and material characterization using nanoindentation methods [19], for example. Even though micro- and nanorobotics have been extensively studied in many application areas, the potential of micro- and nanorobotic technologies has been very inadequately utilized in pulp and paper research.

Paper is a network structure composed of various wood cells, mainly fibers and fines. Fibers are cells having typical dimensions of $0.8 - 4.5\ mm$ in length and $16 - 70\ \mu m$ in diameter depending on their type [20]. Understanding the properties of papermaking fibers will contribute to the understanding of the paper properties as well. For example,

Pooya Saketi is with the Micro- and Nano System Technology group, Department of Automation Science and Engineering of Tampere University of Technology, Korkeakoulunkatu 3, Tampere 33720, Finland, `pooya.saketi@tut.fi`

Arnis Treimanis is with the Latvian Institute of Wood Chemistry, Dzerbenes iela 27, Riga LV 1006, Latvia, `arnis.treimanis@cella.lv`

Pedro Fardim is with the Laboratory of Fibre and Cellulose Technology, Åbo Akademi University, Piispankatu 10, 20500 Turku, Finland, `pfardim@abo.fi`

Pekka Ronkanen is with the Micro- and Nano System Technology group, Department of Automation Science and Engineering of Tampere University of Technology, Korkeakoulunkatu 3, Tampere 33720, Finland, `pekka.ronkanen@tut.fi`

Pasi Kallio is with the Micro- and Nano System Technology group, Department of Automation Science and Engineering of Tampere University of Technology, Korkeakoulunkatu 3, Tampere 33720, Finland, `pasi.kallio@tut.fi`

researchers and engineers are using mathematical models to estimate the microscale properties of pulp and paper [21].

The mechanical properties and chemical composition of papermaking fibers are normally determined by bulk (i.e. average) parameters using sample portions of the fibers under study [22]. The average bulk parameters, however, do not provide a real possibility for predicting relevant fiber properties and chemical composition. The interest in and the necessity of getting new information and data on papermaking fibers and fiber wall fine structures have increased during the recent years. In addition to the new measurement data, controlled mechanical treatment and chemical functionalization of individual paper fibers (IPFs) could lead to dramatic improvements in properties of fiber products. The aforementioned controlled functionalization, treatment and characterization of individual fibers can be studied only by developing new tools. The methods available currently in industrial and academic fiber research laboratories are typically very laborious to use, require extensive manual preparation and provide a very low yield.

Micro- and nanorobotic technology facilitates the development of a novel research platform which will allow the needed versatile fiber studies (e.g. paper fibers, hair, wool, cotton and etc.) at a sufficiently high throughput at an individual cell level in a single instrument. This paper presents a basis for such a versatile microrobotic platform and illustrates fiber flexibility measurement as an example of the operations which will be performed with the platform.

Flexibility is one of the major factors which affects the quality and mechanical properties of paper sheets. Considering the current methods to measure flexibility of individual paper fibers such as measurement of wet fiber flexibility by confocal laser scanning microscopy and single fiber flexibility measurement in a flow cell based device [23]–[25], they are measuring the flexibility of IPFs indirectly. The most important advantage of the approach to be used in the Paper Fiber Manipulation and Mechanical Characterization Platform (PFM&MCP) proposed in this paper is the ability to measure the flexibility of IPFs directly. Two microgrippers are used to grasp an IPF and a known force is applied in the middle of the beam. A both-ends-fixed boundary condition of beam theory [26] is applied to measure the flexibility of an IPF. One-end-fixed or cantilever boundary condition applied for characterization of Carbon-Nanotubes [27] is not suitable for characterization of IPFs due to the curly structure of paper fibers.

Both softwood and hardwood paper fibers are used in the experiments. The wood of angiosperms, flowering plants,

is called hardwood and the wood of gymnosperms, seed-bearing plants, is known as softwood [28]. This is a misnomer as not all hardwoods are necessarily very hard, indeed Ochroma is an example of a very soft hardwood [29].

The rest of the paper is organized as follows. Section II encompasses the objectives of the study and Section III explains the architecture of the proposed PFM&MCP. Next, Section IV analyses the technical requirements of the PFM&MCP. Section V elucidates the design and implementation and Section VI demonstrates the operation of fiber flexibility measurement and the results. Finally, Section VII provides conclusion and discussion on future works.

II. Objectives and Scope of the Study

The objective of the study is to develop a new platform to characterize the flexibility of IPFs using micro and nanorobotics technologies. To provide sufficient amount of data which leads to statistically reliable results, thousands of IPFs should be tested. This platform is aimed for providing an infra-structure to develop a versatile fully automated IPF characterization system which makes this goal achievable. The platform should provide

- means to manipulate and sort IPFs,
- means to measure the flexibility of the IPFs,
- means to prepare samples for other instruments,
- means for chemical treatment of IPFs, and
- an infra-structure for a fully automated PFM&MCP.

III. Conceptual Design

The architecture of the PFM&MCP is illustrated in Fig. 1. It includes six main functions: sample storage, micromanipulation, force sensing, visualization, dispensing and control. Fig. 1 shows these six functions and their interaction to each other. Each function is divided to sub-functions which are explained in this section in details.
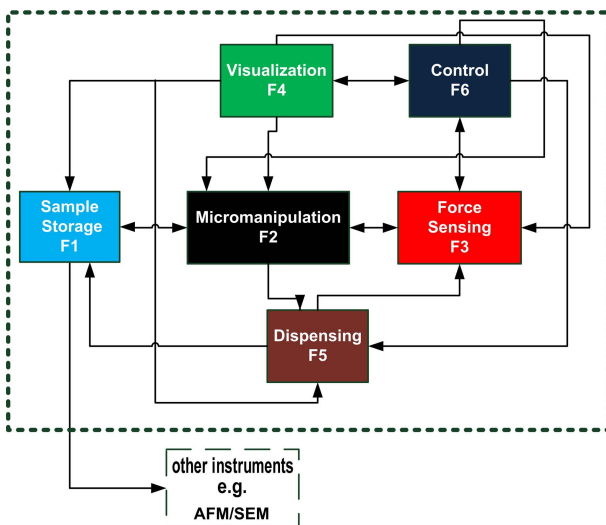

Fig. 1: Main Functions.

A. Sample Storage (F1)

Sample storage (F1) consists of three sub-functions: suspension storage, dry storage and frame fixture. To pick-up and separate IPFs, it is necessary to disintegrate the dry pulp and make the paper fibers float in the water. Fibers are dried and stored in a paper fiber bank. The individual paper fiber bank (IPF-bank) is a place to store the IPFs sorted based on their type, length and treatment for example. The coordinates of the sorted and stored IPFs and their properties are saved for a later use. The platform also prepares samples for other instruments, such as Atomic Force Microscope (AFM) or Scanning Electron Microscope (SEM).

B. Micromanipulation (F2)

Micromanipulation function (F2) enables micropositioning, micro-orienting and microgripping of the IPFs. The micropositioning sub-function is used for placing the area of interest, an IPF-bank, a rotary table, a force sensor, in the working space of microgrippers. Micro-orienting facilitates the change of fiber orientation; and microgripping performs the grasping and handling of IPFs. Micromanipulation is also used for moving the dispenser and aligning the dispenser tip on the required targets to shoot droplets for chemical treatment.

C. Force Sensing (F3)

Force sensing function enables the flexibility measurement. This function measures the magnitude of force, F, which is applied to the IPFs to bend them and uses information from the other functions such as the length of IPFs, L, from the visualization function (F4) in the control system, to measure the flexibility of IPFs.

D. Visualization (F4)

Visualization function (F4) is composed of four sub-functions: imaging, magnification, illumination and signal analysis. Imaging sub-functions acquire visual information to be used as visual feedback in the control function (F6). Since IPFs with the dimensions alluded in Table I are to be characterized in the platform, a sufficient magnification and high quality illumination are essential. To accomplish pattern recognition and image analysis as quickly as possible, an independent signal analysis sub-function is required.

E. Dispensing (F5)

Dispensing (F5) encompasses two sub-functions, preparatory-chemical treatment which is required in the sample storage function (F1); and instant chemical treatment which is useful when chemical treatment is needed before the flexibility measurement test.

TABLE I: Paper Fiber Dimensions [20].

	Length (mm)	Diameter (μm)
Hardwood	0.8 - 1.6	16 - 25
Softwood	2 - 4.5	20 - 70

F. Control (F6)

The most important sub-function of the control function (F6) is the micromanipulation control which controls micropositioning, micro-orienting and microgripping devices. Visualization control sub-function regulates zooming and fine focusing. A user interface sub-function connects all the control sub-functions to the human operator. Force feedback sub-function supplies a sensible force feedback to the human operator. Dispensing control sub-function triggers the dispenser and provides the required droplet size for chemical treatment. The required calculations to measure the flexibility of the IPFs are performed in the measurement algorithm sub-function.

IV. TECHNICAL REQUIREMENTS

In this section, the survey and selection of devices used to implement the micromanipulation, visualization and force sensing functions in the platform are briefly explained. The major technical requirements for micromanipulation, visualization and force sensing functions stem from the IPF dimensions and throughput objectives.

Whereas characterizing few IPFs is not sufficient to provide valuable statistical information about paper fibers, it is necessary to perform these characterization tests automatically. Based on wood scientists' requirements, five thousand tests per day, 24 hours, provides adequate amount of data for statistical analysis. We reserve a 6 hours calibration and maintenance break for a day; this leaves $13s$ for each experiments. We have identified six tasks in a flexibility measurement procedure, *IPF recognition and coordinate calculation, IPF orientation and pick-up, IPF length measurement, IPF transport to force sensing place, chemical treatment and force sensing and calculation*; providing and average of $2.16s$ for each task.

A. Micromanipulation

The micropositioning, micro-orienting and microgripping sub-functions are implemented by using a two degrees-of-freedom (DOF) micropositioner (MP), a rotary table and two microgrippers mounted on XYZ-micropositioners, respectively.

The technical requirements of the aforementioned sub-functions are shown in Table II which are derived based on the average time of each task, minimum and maximum diameter of IPFs, accessibility of MP to all sections of the platform, the required travel directions, the required resolution and speed, and the accessibility of microgrippers (MG)s to the rotary table, the IPF-bank and the force sensor.

TABLE II: Technical Requirements of Micromanipulation.

	Resolution	Direction	Speed	Travel
μ-positioning	sub-μm	XY	9.1 mm/s	4cm
μ-orienting[1]	10 $\mu°$	CW-CCW	$30°/s$	$90°$
μ-gripping[2]	sub-μm	XYZ-Gripping	9.1 mm/s	2 cm

1) Diameter: Min.1 cm
2) Gripper Tip Opening: Min. $70\mu m$, Max. 1 mm

B. Visualization

For the PFM&MCP applications, a high optical resolution is necessary to achieve detailed images. Based on the IPF dimensions, the required Field of View (FOV) is around $4.5 \times 2 \ mm^2$. In another hand, a broad image of the test bench and MGs is also needed which requires a larger FOV such as $20 \times 8 \ mm^2$. To have a proper image of the paper fibers $3X$ magnification is required. To have the broad image of the working space $0.25X$ magnification is required leading to a magnification range of $0.25X - 3.00X$. Since a wide range of magnification is needed, a zooming tube microscope is preferred to a constant magnification tube microscope. To know the magnitude of the zoom to estimate the length of paper fiber, a computer controlled motorized zooming system is needed. Considering the size of XYZ-micropositioners, the required working distance of the tube microscope is minimum $5 \ cm$. In flexibility measurement application where only the length of the IPF is measured from the image, the required spatial resolution for the camera is calculated to be $5.00 \ \mu m$ or better.

C. Force Sensing

This section explains the technical requirements of force sensor needed for flexibility measurement of IPFs. To select a suitable micro force sensor it is necessary to estimate the amplitude of force to measure the flexibility of IPFs by using simulation techniques. Since two MGs are used to grasp the IPFs, the both end fixed boundary conditions of beam theory are applicable in this case [26]. Since the applied force, F, is in the middle of the beam, the IPF, the simplified beam equation is as follows:

$$y = \frac{-FL^3}{192EI} \qquad (1)$$

where y, L, E and I are deflection, length, Young's modulus and moment of inertia, respectively. Flexibility is the compliance of an elastic body to deformation by an applied force,

$$Flexibility = \frac{1}{EI} = \frac{-192y}{FL^3} \qquad (2)$$

Regarding to the fact that cellulose is the main material in a paper fiber cell wall, it is possible to use the Young's modulus of microcrystalline cellulose, $25 \pm 4GPa$ [30], the geometry of hardwood and softwood, Table I, and Equation 2 to simulate the required forces to bend an IPF. The simulation shows that the maximum required forces for hardwood and softwood are $206\mu N$ and $29\mu N$, respectively. Table III shows the flexibility values based on the Young's modulus of microcrystalline cellulose and IPF dimensions of Table I. In this simulation, it is assumed that the maximum deflection, y, is 2% of the length of the IPFs.

V. DESIGN AND IMPLEMENTATION OF THE PLATFORM

Considering the technical requirements of the visualization function, a motorized zoom system providing $0.29X - 3.50X$ magnification and LED coaxial illumination are chosen (Navitar Co.). The camera (XCD-U100 Sony) selected has

TABLE III: Flexibility Values based on the Young's modulus of Microcrystalline Cellulose ($E = 25 \pm 4GPa$) [30]. Assumption: Maximum Deflection is 2% of the Length of the IPFs.

	Bending Stiffness $(Nm^2) \times 10^{-9}$	Flexibility $(N^{-1}m^{-2}) \times 10^9$
Softwood	29.710	0.337
Hardwood	12.796	7.815

a $1/1.8$" CCD cell chip, a resolution of $1600 \times 1200 pixel$ and a pixel size of $4.4\mu m$.

After several design iterations, a "Stacked Gantry Crane" configuration, shown in Fig. 2, is used in the platform. It provides several benefits, such as having the most compact design without coordinate mapping and with fixed camera. Table IV shows the components of PFM&MCP based on numbering of Fig. 2. In this configuration, there is one tailored 4DOF (1), and one 5DOF (2) micromanipulator from SmarAct Co. In addition to the XYZ-positioners and the MG, the 5DOF unit includes a positioner for a dispenser (3). The platform includes also a XY-Table (5) of SmarAct on top of which the following equipment are mounted: force sensor (FT-S540 of Femtotools) (7), a micro-rotary table (SR-1908 of SmarAct) (4), and the IPF-bank (6) to perform the designed tasks. The IPF-bank is made of SU-8, a common epoxy-based negative photoresist polymer used in lithography, with the height of $200\mu m$ and placed on XY-Table to store the sorted IPFs.

The functions for the flexibility measurement of IPF has been implemented. Fig. 3 and 4 show the top and side view of the current implementation of the platform, respectively.

VI. EXPERIMENTS AND RESULTS

Softwood, hardwood and treated softwood are used as raw materials in the experiments. The first sample, Sample 1, is bleached Pine kraft pulp which is softwood. The second sample, Sample 2, is bleached hardwood pulp. A paper fiber
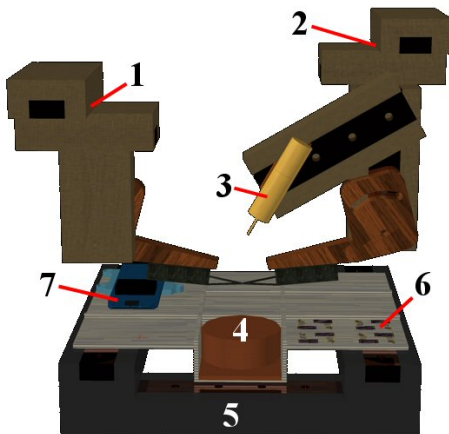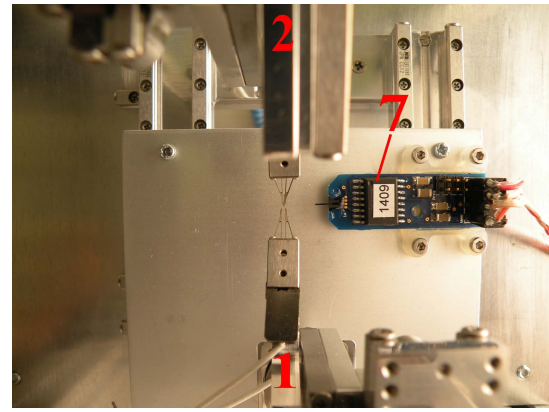

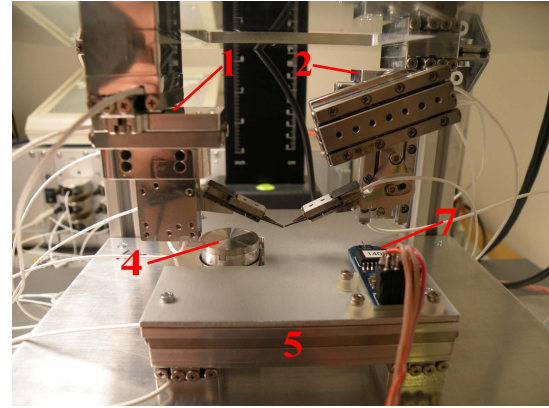Fig. 3: Assembled PFM&MCP while Operation - Top View.

Fig. 4: Assembled PFM&MCP in Operation - Side View.

cell consists of four walls; middle lamella, ML, which is usually destructed during pulping and bleaching operations totally; primary wall, P; secondary wall consisting of S1, S2 and S3 layers; and cell lumen which is void. As an additional challenge, Sample 1 is treated such that the S2 and S3 layers and also residues of S1 layer remain in the cell wall, providing us Sample 3. Fig. 5 shows the wood cell wall structure.

A small bundle of paper fibers is taken from the pulp sample. The bundle is placed in a Petri dish and it is disintegrated by adding deionized water and shaking. Then the IPFs are soaked for five minutes. Next, the IPFs are placed on the rotary-table by using a pipette.

Fig. 6 illustrates the process of flexibility measurement in the teleoperation mode. The IPFs are initially in the wet state and they are placed on the rotary-table. The MGs are

Fig. 2: 3D Design of PFM&MCP.

TABLE IV: Components of PFM&MCP.

No.	Component	DOF	Comments
1	Microgripper (1)	4	XYZ + Gripping
2	Microgripper (2)	5	XYZ + Gripping + Dispenser Positioning
3	Dispenser	-	Performing Chemical Treatment
4	Rotary Table	1	Rotation in XY-Plan
5	Micropositioner	2	XY-Table
6	IPF Bank	-	Storing and Sorting of IPFs
7	Force Sensor	-	Capacitive Microforce Sensor
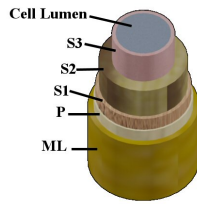
Fig. 5: Wood Cell Wall Structure. ML: Middle Lamella, P: Primary Wall, S1-S3: Secondary Wall Layers [31].

Fig. 7: Force - Displacement Graph.

used to pick up the selected IPF from the both ends, (1 & 2), and lift it synchronizedly. The MGs straighten the IPF by pulling it in continuous $5\mu m$ steps until it reaches to the slippage limit of the MGs, (3 & 4). The length, L, of IPF is measured using the vision system. After picking up the IPFs, the fibers are kept in $27 \pm 2\%$ humidity and $25 \pm 1°C$ for five minutes before starting the measurements. Then the force sensor is pushed into the middle of the IPF by using the XY-Table and to acquire the force F, (5 & 6). The deflection, y, of the center point of IPF is read out from the position sensor of the XY-Table. The IPF and the force sensor probe are aligned in z-direction by using the depth of the focus method. The force sensor signal is also used to stop the test, if the applied force exceeds 100% of full scale. By substituting the three measured parameters, L, F and y, into Equation 2, it is possible to calculate the flexibility of the IPF. Fig. 7 shows and demonstrates that there is no slippage of the IPF in the measurement process within the force sensor working range. Fig. 7 also illustrates the force recorded based on $1\mu m$ increase in the deflection of an IPF; meaning that the experiments are performed in the elastic region of stress-strain curve. Table V summarizes the results of the experiments by giving average values of ten measured fibers and their standard deviations.

VII. CONCLUSIONS AND FUTURE WORK

A. Discussions and Conclusions

Table V shows that hardwood IPFs have a higher flexibility compared to softwood IPFs. The hardwood/softwood flexibility ratio based on simulation and experiments are 23.22 and 21.86, respectively; which indicates similar ratio of flexibility values [See Table V and Table III]. The IPF model used
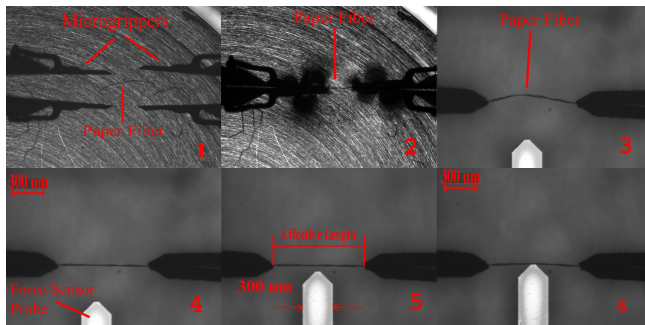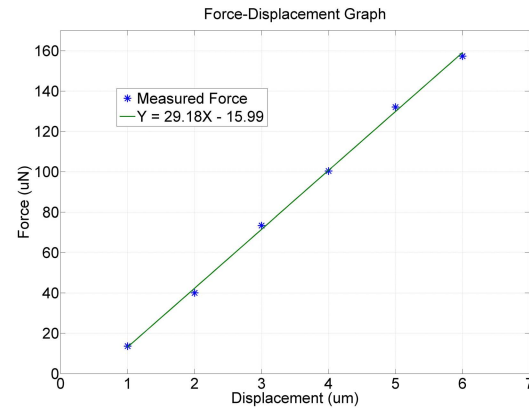
in the simulation is a symmetrical tube but the real IPFs are natural fibers which are asymmetric and they have structural disorders. Furthermore, the simulation assumes that the paper fiber cell wall is made of homogeneous cellulose; but it also contains hemicellulose and lignin in addition to cellulose. Therefore, the results based on simulation differ from the average results based on experiments but they have similar hardwood/softwood flexibility ratio.

Although the average flexibility values of treated softwood fibers seems to differ from the normal softwood, the high standard deviation prevents the flexibility comparison between the two samples.

The IPFs used in the aforementioned tests are pulp fibers and not wood fibers. The pulping process damages the IPF's body seriously. It is difficult to distinguish and to categorize the IPFs of pulp fibers. Wood fibers, however, are screened manually based on their botanical properties, such as latewood or earlywood, fibers or tracheids, etc. This issue is one of the main sources of errors in these measurements.

A novel microrobotic platform for flexibility measurement of individual paper fibers is developed and the method is validated in the experiments. The experiments indicate that the hardwood fibers have higher flexibility values than softwood fibers.

B. Future Work

In the continuation of this project the following actions can be taken.

Fig. 6: PFM&MCP while Flexibility Measurement.

TABLE V: Results

TEST	Bending Stiffness $(Nm^2) \times 10^{-9}$	Flexibility $(N^{-1}m^{-2}) \times 10^9$	Eff. Length* (μm)
Softwood (n=10)	0.12 ± 0.042	9.37 ± 0.042	1267 ± 267
Hardwood (n=10)	0.0077 ± 0.0044	204.83 ± 170.19	321 ± 75
Softwood - S2S3 (n=10)	0.29 ± 0.24	7.63 ± 6.93	1366 ± 407

*Eff. Length: Effective Length is the free length of IPF between two MGs.

The aforementioned tests need to be repeated by using wood fiber samples instead of pulp fiber samples.

A controlled humidity and temperature chamber will be added to the platform, because the standard conditions for testing the IPFs require $50\% \pm 2$ relative humidity and $20 \pm 1^\circ C$ temperature.

The preliminary flexibility tests with softwood IPFs under axial tension show improvements in the repeatability of the results but the mathematical model which includes the effect of the axial tension needs to be incorporated. It is necessary to integrate an axial force sensor into the PFM&MCP, to measure the actual flexibility of the IPFs under simultaneous axial and transverse loading.

To collect statistically reliable information, it is necessary to make aforementioned teleoperated process in Section VI and Fig. 6 fully automated in the future to perform hundreds of flexibility tests per hour. On the other hand, this platform can be used not only for IPFs but also for other kinds of fibers in microscale.

VIII. ACKNOWLEDGMENTS

REFERENCES

[1] F. Krohs, S. Hagemann, S. Fatikow, "Automated Cell Characterization by a Nanohandling Robot Station", *Mediterranean Conference on Control & Automation*, 27-29 June 2007, Athens, Greece, pp 1-6.

[2] K. Sakaki, N. Dechev, E.J. Park, R.D. Burke, "Development of a Five Degree-Of-Freedom Biomanipulator for Autonomous Single Cell Electroporation", *IEEE/RSJ International Conference on Intelligent Robots and Systems*, Oct. 29-Nov. 2 2007, San Diego, USA, pp 3137-3143.

[3] H. Matsuokaa, T. Komazakia, Y. Mukaia, M. Shibusawaaa, H. Akanea, A. Chakic, N. Uetakec and M. Saitoa, "High Throughput Easy Microinjection with a Single-Cell Manipulation Supporting Robot", *Journal of Biotechnology*, Vol. 116, No. 2, 2005, pp 185-194.

[4] K. Kim, X. Liu, Y. Zhang and Y. Sun, "Nanonewton Force-Controlled Manipulation of Biological Cells Using a Monolithic MEMS Microgripper with Two-Axis Force Feedback", *Journal of Micromechanics and Microengineering*, Vol. 18, No 5, 2008, 8pp.

[5] W. Wang, X. Liu, D. Gelinas, B. Ciruna and Y. Sun, "A Fully Automated Robotic System for Microinjection of Zebrafish Embryos", *PLoS ONE*, Vol. 2, No. 9, Sep. 2007, e862.

[6] J. Park, S-H. Jung, Y-H. Kim, K. Byungkyu, S-K. Lee, B. Ju and K-I Lee, . "An Integrated Bio Cell Processor for Single Embryo Cell Manipulation", *IEEE/RSJ International Conference on Intelligent Robots and Systems*, Sep. 28-Oct. 2 2004, Sendai, Japan, pp 242-247.

[7] E. W. H. Jager, O. Ingans, I. Lundstrm, "Microrobots for Micrometer-Size Objects in Aqueous Media: Potential Tools for Single-Cell Manipulation", *Science Magazine*, Vol. 288, No. 5475, 2000, pp 2335-2338.

[8] J. P. Desai, A. Pillarisetti and A. D. Brooks, "Engineering Approaches to Biomanipulation", *Annual Review of Biomedical Engineering*, Vol. 9, No. 1, Mar. 2007, pp 35-53.

[9] Y. Sun, M.A. Greminger and B.J. Nelson, "Investigating Protein Structure with a Microrobotic System", *IEEE International Conference on Robotics and Automation*, Apr. 26 - May 1 2004, New Orleans, USA, pp 2854-2859.

[10] F. Arai, T. Sakami, H. Maruyama, A. Ichikawa and T. Fukuda, "Minimally Invasive Micromanipulation of Microbe by Laser Trapped Micro Tools", *IEEE International Conference on Robotics and Automation*, 11-15 May 2002, Washington DC, USA, pp 1937-1942.

[11] A. Georgiev, P.K. Allen and W. Edstrom, "Visually-guided Protein Crystal Manipulation using Micromachined Silicon Tools", *IEEE/RSJ International Conference on Intelligent Robots and Systems*, Sep. 28-Oct. 2 2004, Sendai, Japan, pp 236-241.

[12] K. Inoue, T. Arai, T. Tanikawa and K. Ohba, "Dexterous Micromanipulation Supporting Cell and Tissue Engineering", *IEEE International Symposium on Micro-NanoMechatronics and Human Science*, 7-9 Nov. 2005, Nagoya, Japan, pp 197-202.

[13] J. Hirvonen, P. Ronkanen, T. Ylikomi, M. Bluer, R. Suuronen, H. Skottman & P. Kallio "Microcutting of Living Tissue Slices and Stem Cell Colonies by Using Mechanical Tool and Liquid Jet", *Proceedings of the 2nd IEEE/RAS-EMBS International Conference on Biomedical Robotics and Biomechatronics*, 19-22 Oct. 2008, Scottsdale, Arizona, USA, pp 612-617.

[14] P. Kallio and J. Kuncova, "Capillary Pressure Microinjection of Living Adherent Cells: Challenges in Automation", *Journal of Micromechatronics*, Vol. 3, No. 3-4, 2006, pp 189-220.

[15] P. Kallio, T. Ritala, M. Lukkari & S. Kuikka, "Injection Guidance System for Cellular Microinjections", *The International Journal of Robotics Research, Sage Publications, special issue on First IEEE/RAS-EMBS International Conference on Biomedical Robotics and Biomechatronics 2006*, Vol. 26, No. 11-12, 2007, pp 1303 - 1313.

[16] K. Carlson, K. N. Andersen, V. Eichhorn, D. H. Petersen, K. Molhave, I. Y. Y. Bu, K. B. K. Teo, W. I. Milne, S. Fatikow. and P. Boggild, "A Carbon Nanofibre Scanning Probe Assembled using an Electrothermal Microgripper", *Journal of Nanotechnology*, Vol. 18, No. 34, 2007, 7pp.

[17] V. Eichhorn, K. Carlson, K.N. Andersen, S. Fatikow and P. Boggild, "Nanorobotic Manipulation Setup for Pick-and-Place Handling and Nondestructive Characterization of Carbon Nanotubes", *IEEE/RSJ International Conference on Intelligent Robots and Systems*, Oct. 29-Nov. 2 2007, San Diego, USA, pp 291-296.

[18] O. Sardan, V. Eichhorn, D. H. Petersen, S. Fatikow, O. Sigmund and P. Boggild, "Rapid Prototyping of Nanotube-Based Devices using Topology-Optimized Microgrippers", *Journal of Nanotechnology*, Vol. 19, No. 49, 2008, 9pp.

[19] W.T.Y. Tze, S. Wang, T.G. Rials, G.M. Pharr, S.S. Kelley, "Nanoindentation of Wood Cell Walls: Continuous Stiffness and Hardness Measurements", *Journal of Composites Part A: Applied Science and Manufacturing*, Vol. 38, No. 3, 2007, pp 945-953.

[20] C. Ververis, K. Georghiou, N. Christodoulakis, P. Santas and R. Santas, "Fiber Dimensions, Lignin and Cellulose Content of Various Plant Materials and their Suitability for Paper Production", *Journal of Industrial Crops and Products*, Vol. 19, No. 3, 2004, pp 245-254.

[21] K. Hofstetter, E. K. Gamstedt, "Hierarchical Modelling of Microstructural Effects on Mechanical Properties of Wood.", *Holzforschung*, Vol. 63, No. 2, 2009, pp 130-138.

[22] S. E. Stanzl-Tschegg, P. Navi, "Fracture Behaviour of Wood and its Composites.", *Holzforschung*, Vol. 63, No. 2, 2009, pp 139149.

[23] D. Yan and K. Li, "Measurement of Wet Fiber Flexibility by Confocal Laser Scanning Microscopy", *Journal of Materials Science*, vol. 43, No. 8, Apr. 2008, pp 2869–2878.

[24] M. Tchepel1, J. W. Provan, A. Nishida and C. Biggs, "A procedure for measuring the flexibility of single wood-pulp fibres", *Journal of Mechanics of Composite Materials*, vol. 42, No. 1, Mar. 2006, pp 83-92.

[25] R. Eckhart, M. Donoser, and W. Bauer, "Single Fibre Flexibility Measurement in a Flow Cell Based Device", *In Proceedings of Advances in Paper Science and Technology (FRC)*, 2009.

[26] W. C. Young and R. G. Budynas, *"Roak's Formulas for Stress and Strain-Seventh Edition"*, ISBN 0-07-121059-8, McGRAW-Hill, 2002.

[27] L. X. Dong, F. Arai, and T. Fukuda, "Destructive Constructions of Nanostructures with Carbon Nanotubes through Nanorobotic Manipulation", *IEEE/ASME Transactions on Mechatronics*, vol. 9, No. 2, Jun. 2004, pp 350–357.

[28] J. D. Mauseth, *"Botany-An Introduction to Plant Biology-3rd Edition"* ISBN:0763721344, Jones and Bartlett Publishers Inc., 2003.

[29] T. Porter, *"Wood: Identification and Use"* ISBN:1861083777, Publisher: Guild of Master Craftsman Publications Ltd, 2004.

[30] S.J. Eichhorn and R.J. Young, "The Young's Modulus of a Microcrystalline Cellulose", *Journal of Cellulose*, vol. 8, No. 3, Sept. 2001, pp 197–207.

[31] J. M. Dinwoodie, *"Wood: Nature's Cellular, Polymeric Fibre-Composite"* ISBN:0901462357, Publisher: Maney Publications, 1989.